Asymmetry-induced particle drift in a rotating flow

J. J. Bluemink, E. A. van Nierop, and S. Luther
Faculty of Science and Technology and J M Burgers Centre for Fluid Dynamics, University of Twente, P.O. Box 217, 7500 AE Enschede, The Netherlands

N. G. Deen
Faculty of Science and Technology, University of Twente, P.O. Box 217, 7500 AE Enschede, The Netherlands

J. Magnaudet
Institute de Mécanique des Fluides de Toulouse (IMFT), 1 Allée du Professeur Camille Soula, 31400 Toulouse, France

A. Prosperetti
Faculty of Science and Technology and J M Burgers Centre for Fluid Dynamics, University of Twente, P.O. Box 217, 7500 AE Enschede, The Netherlands
and Department of Mechanical Engineering, Johns Hopkins University, Baltimore, Maryland 21218

D. Lohse[a)]
Faculty of Science and Technology and J M Burgers Centre for Fluid Dynamics, University of Twente, P.O. Box 217, 7500 AE Enschede, The Netherlands

(Received 11 October 2004; accepted 1 March 2005; published online 11 July 2005)

We report on an intriguing phenomenon taking place in a liquid rotating around a fixed horizontal axis. Under suitable conditions, bubbles and particles are observed to drift along the axis of rotation maintaining a constant distance from it and a constant angle of elevation above the horizontal. Absence of fore-aft symmetry of the bubble or particle shape is a prerequisite for this phenomenon. For bubbles, this requires a volume sufficiently large for surface-tension effects to be small and large deformations to be possible. Particle image velocimetry and flow visualization suggest that the wake does not play a role. The dependence on bubble radius, particle shape, liquid viscosity, and speed of rotation is investigated. © *2005 American Institute of Physics*. [DOI: 10.1063/1.1978921]

INTRODUCTION

In the course of an ongoing project to study the forces acting on bubbles in a rigid-body rotating flow, we encountered an intriguing phenomenon which is reported in this paper. In the experiment, a liquid-filled horizontal glass cylinder (length of 500 mm, diameter of 100 mm) is in steady rotation around its axis. Under certain conditions, a large bubble (equivalent radius $R_b > 5$ mm) injected in the liquid starts moving back and forth along a line parallel to the axis of the cylinder, without any external force acting in this direction, while maintaining a constant distance from the axis and elevation from the horizontal. Further experiments indicate that certain particles also exhibit a similar axial drift.

DRIFTING BUBBLES

The cylinder is filled with a glycerin-water mixture and maintained in steady rotation with angular velocities ω between 0 and 40 rad s^{-1}. In this flow, small bubbles (bubble radius $R_b \approx 1$ mm) reach a steady equilibrium position under the action of buoyancy, drag, added mass, and lift.[1,2] In a water-glycerin mixture with relatively large viscosity ($\nu \geqslant 10^{-5}$ m^2 s^{-1}) and at sufficiently large angular velocities, on the other hand, large bubbles (equivalent bubble radius 5 mm $\leqslant R_b \leqslant$ 10 mm) are observed to drift parallel to the cylinder axis, see Fig. 1(a). Their shape has no obvious symmetry. The drift appears to be very regular and steady and to take place at a fixed distance r_e from the axis of rotation and at a fixed angle of elevation φ_e above the horizontal. When the bubble reaches an end cap of the cylinder, it bounces, its shape is reflected, and it starts traveling in the opposite direction at the same speed as before. At lower viscosities, these large bubbles tend to break and, when they do not, their translational motion in general is less stable. If the bubble is too large ($R_b \geqslant 15$ mm) or the rotation rate is too high, the bubble also breaks.

The drift velocity v_z is found to be dependent on the angular velocity ω, the equivalent bubble radius R_b, and the liquid viscosity. Figure 1(b) shows v_z versus the rotation rate for different R_b and ν.

A first obvious hypothesis as to the nature of this phenomenon is a large-scale flow caused by Ekman layer pumping due, perhaps, to the presence of a Taylor column (of length $\sim R_b^3 \omega / \nu$) produced by the bubble. This possibility is however easily dismissed as small particles present in the liquid away from the bubble did not exhibit any axial motion. Furthermore, estimates of the length of a possible Taylor column are at most a few centimeters, much less than the length of the cylinder. Ekman layer pumping may, however, help in making the bubble bounce at the end caps of the cylinder.

[a)]Author to whom correspondence should be addressed. Electronic mail: d.lohse@tnw.utwente.nl

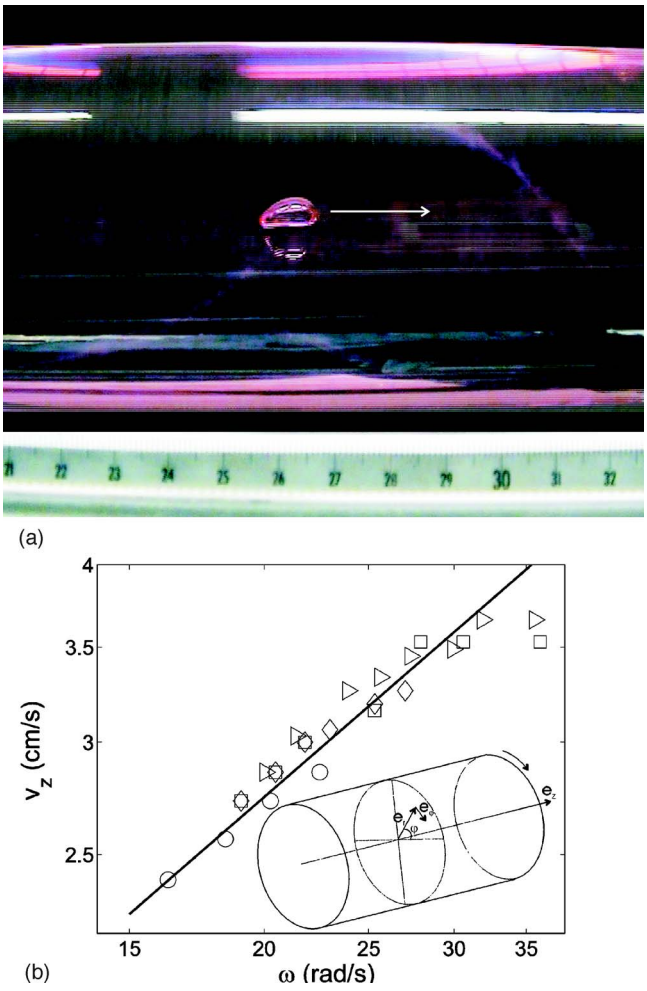

FIG. 1. (a) A photograph of the experiment with the drifting bubble. The scale is in cm. (b) The axial drift velocity vs the rotation rate of the cylinder for large bubbles on a log-log scale. □ $R_b \approx 6.2$ mm, ○ $R_b \approx 7.2$ mm; ▷, ◇ R_b not specifically measured. □ $\nu = 6.7 \times 10^{-5}$ m^2 s^{-1}; ○, ▷, and ◇ $\nu = 1.7 \times 10^{-5}$ m^2 s^{-1}. Solid line: $v_z \propto \omega^{0.66}$. The inset shows the coordinate system. [Enhanced online; (a) links to a real-time movie of the drifting bubble.]

In order to gain some understanding of the nature of the flow near the bubble, the liquid was seeded with tracer particles illuminated by a light sheet perpendicular to the cylinder axis in a standard particle image velocimetry (PIV) arrangement. Figure 2 shows a cross section of the disturbance velocity field around the bubble, the undisturbed velocity field being estimated assuming solid-body rotation. Here the rotational Reynolds number, defined as $\mathrm{Re}_r = \omega r_e R_b / \nu$ is about 20. The x axis is horizontal and the y axis vertical in a plane perpendicular to the cylinder axis, which goes through ($x=0$, $y=0$) and which is marked by the cross. The magnitude of the velocity vectors is represented both by their length and the color coding. Due to the subtraction of the solid-body rotational velocity, the figure is a representation of the velocity field in the rotating frame. Thus, the image must be interpreted as showing a bubble moving (counterclockwise) in an essentially quiescent liquid. The velocity ahead of the bubble is seen to be very small, suggesting that the wake trailing the bubble in the circular motion has essentially dissipated by the time the liquid has completed an entire revolution. Thus, the bubble does not seem to interact appreciably with its own wake.

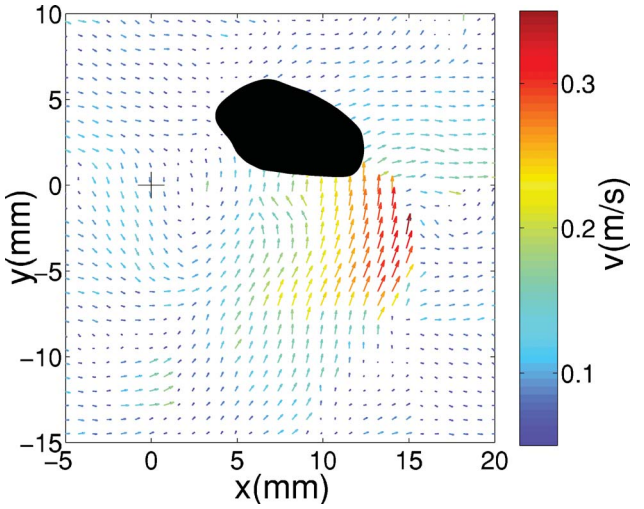

FIG. 2. (Color). Difference between the velocity fields with and without the bubble in a plane perpendicular to the cylinder axis; the bubble (black silhouette) is moving towards the camera. $\omega = 22.6$ rad/s, $\nu = 9.9 \times 10^{-5}$ m^2/s, and $R_b = 8$ mm.

By recording the tracer particles trajectories with a longer exposure we obtain an indication of the path-lines of the flow. In Fig. 3 the path-lines in a cross section of the (x,y) plane are shown for a bubble moving away from the camera. Here several vortices are apparent, although it is not clear whether they remain attached to the bubble or are shed similarly to a Kármán vortex street. The relatively low Reynolds number of the rotational flow, $\mathrm{Re}_r \sim 20$, suggests the first possibility as the more likely one.

DRIFTING PARTICLES

Since the phenomenon only occurs with strongly deformed bubbles, we decided to investigate whether it would also occur with asymmetrically shaped rigid bodies made out of a plastic material with a density $\rho = 900$ kg m^{-3}. As a control, we used particles with fore-aft symmetry such as solid

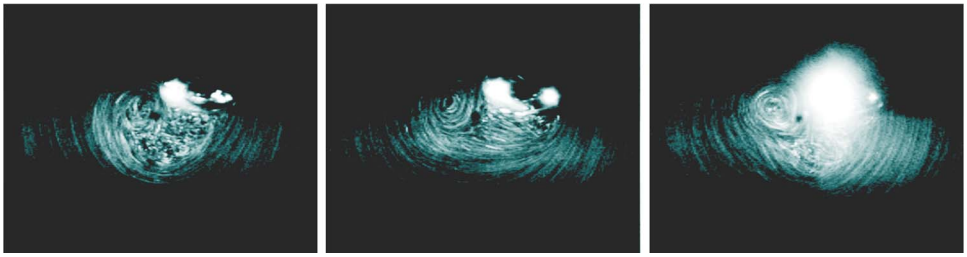

FIG. 3. Path-lines in (x,y) plane around a bubble moving through a light sheet away from the camera. $\omega = 28.3$ rad/s, $\nu = 1.8 \times 10^{-4}$ m^2/s, and $R_b = 10$ mm.

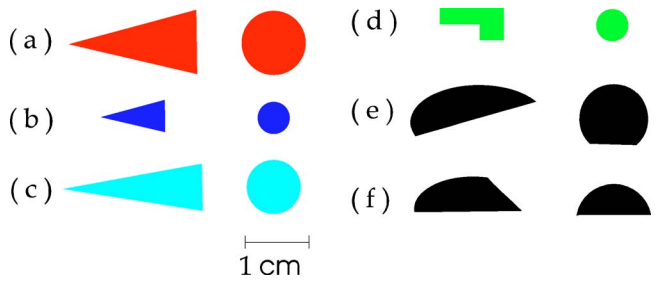

FIG. 4. Particles that display axial drift in rigid-body rotation. Side view (left) and top view (right). The legends in Figs. 5–8 refer to the letters in this figure.

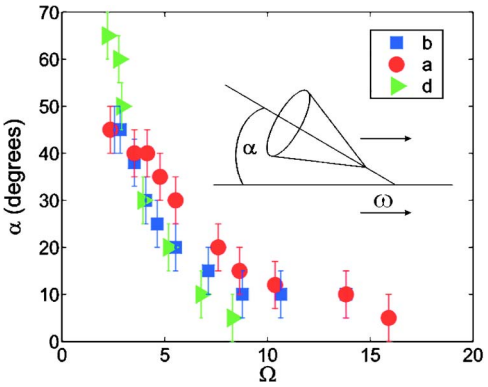

FIG. 5. Tilt of the particle with respect to the cylinder axis (α) vs Ω. The tilt is determined with a protractor, which accounts for the rather large error.

spheres, prolate spheroids, and cylinders and spheroids cut by planes parallel to the major axis. All these symmetric bodies aligned their major axes with that of the rotating cylinder and came to an equilibrium position (fixed r_e, φ_e, and axial location) just like spherical bubbles. When the fore-aft symmetry is broken, however, the same axial drift observed with large bubbles sets in. The presence or absence of axial symmetry did not seem to play a role. Thus, we find that cones [Figs. 4(a)–4(c)] exhibit axial drift, as well as "mutilated" cylinders [Fig. 4(d)], and spheroids cut at an angle to their symmetry axis [Figs. 4(e) and 4(f)]. The linear dimensions of the particles we studied were of the order of 10 mm and the angular velocities for which the drift occurred were substantially lower than for bubbles, between 2 and 20 rad s^{-1}. Unlike bubbles, for particles the axial drift was found in fluids with both high and low viscosities (e.g., water); however, the phenomenon was robust when $\nu \geqslant 10^{-5}$ m^2 s^{-1}. In addition, in contrast to bubbles, which are observed to turn around once they reach one of the bases of the cylinder, solid particles remain at the bases—a behavior which agrees with the idea that the reflection of the bubble shape is directly responsible for the change of sign of the axial velocity.

We characterize the size of the particles in terms of the radius of the base shown in the right column of Fig. 4; this characteristic length will be denoted by the same symbol R_b used earlier for the equivalent bubble radius. Given the variables ω, ν, R_b, and the gravitational acceleration g, two nondimensional parameters can be defined, a "Froude number" $\mathrm{Fr}=\omega^2 R_b/g$ and a dimensionless angular velocity $\Omega=\omega R_b{}^2/\nu$. This latter parameter represents the square of the ratio of the particle radius to the viscous diffusion length. The response of the system can be characterized in terms of the rotational Reynolds number Re_r defined earlier, the drift Reynolds number $\mathrm{Re}_d=v_z R_b/\nu$, and the angle of tilt α of the particle with respect to the cylinder axis.

Figure 5 shows the tilt angle α vs Ω for a glycerin-water mixture of 80% glycerin by weight. The particles only tend to align with the cylinder axis at high rotation rates, while at low rotation rates the tilt can be quite substantial. The particles display the largest drift velocity when their angle of tilt is between 20° and 40°.

In Fig. 6 the drift Reynolds number Re_d is plotted as a function of the dimensionless numbers Ω and Fr for particles of different size and shape, and for different viscosities. The cut cylinder and small cone have the same base surface, while the base surface of the large cone is twice as large. The aspect ratios for all particles in the figure is 2:1. The cones follow their tips, the cut cylinder follows the side where the material is cut away.

It was already mentioned that the particle drift depends on the liquid viscosity. Figure 6 shows the drift Reynolds number of the particles in glycerin-water mixtures of 60% and 80% by weight versus Ω [Fig. 6(a)] and versus Fr [Fig. 6(b)]. The straight lines in Fig. 6(a) correspond to $\mathrm{Re}_d \sim 1/\Omega^2$ or $v_z \sim \nu^3/(\omega^2 R_b^5)$, while the straight lines in Fig. 6(b) show the relation $\mathrm{Re}_d \sim \mathrm{Fr}^{-1}$ or $v_z \sim \nu g/(\omega^2 R_b^2)$. These

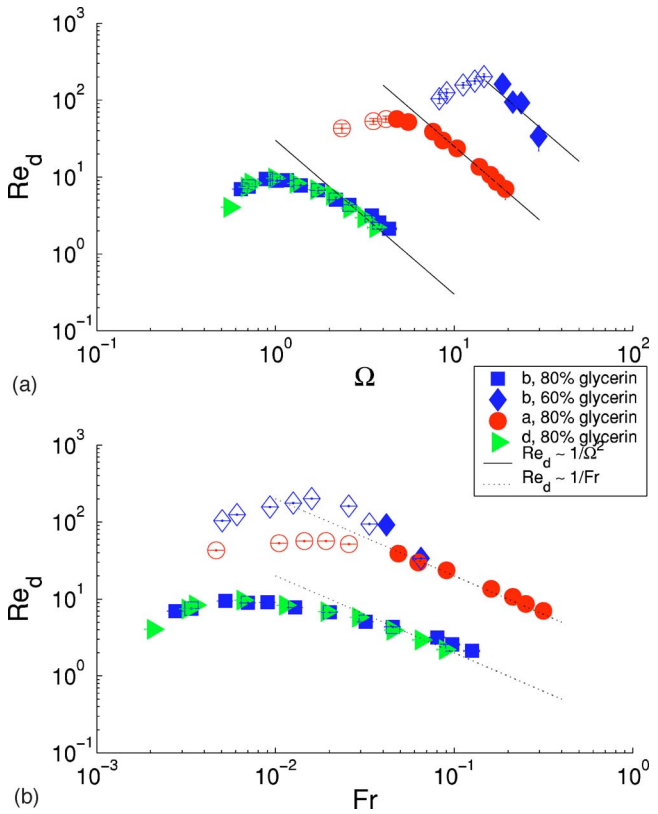

FIG. 6. Drift Reynolds number vs (a) $\mathrm{Re}_d=\omega R_b{}^2/\nu$, and (b) $\mathrm{Fr}=\omega^2 R_b/g$ for cones moving in the direction of the tip. Open symbols: data for particles estimated to be near the cylinder wall.

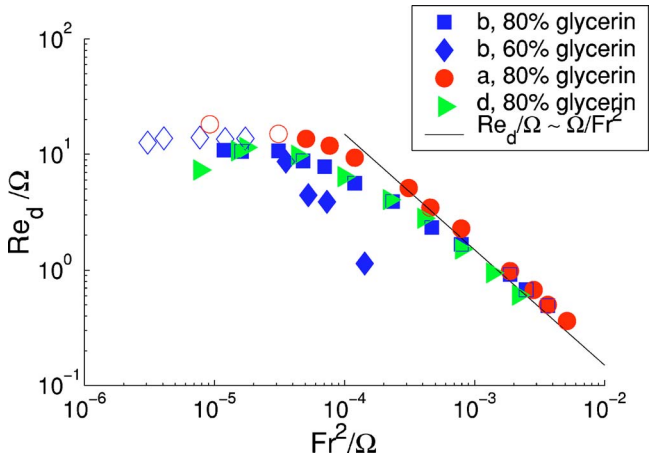

FIG. 7. Scaled drift Reynolds number Re_d/Ω vs Fr^2/Ω for cones moving in the direction of the tip.

figures seem to exhibit two different regimes, one for the lower values of Ω or Fr, and one for larger values of these quantities.

In Fig. 7 the same data are plotted in the form of Re_d/Ω vs Fr^2/Ω. This figure indicates that, for sufficiently large values of the parameter Fr^2/Ω and the larger viscosity, the results for Re_d/Ω exhibit an approximate collapse onto a line $\mathrm{Re}_d/\Omega \sim \Omega/\mathrm{Fr}^2$, implying $v_z \sim g^2 R_b/(\nu\omega^2)$.

It seems that the direction of motion depends on the orientation of the particle: The tip seemed to be inclined towards the axis of rotation, when the drift was in the direction of the tip. For drift in the opposite direction, the tip seemed to be oriented away from the axis. If the orientation is reversed by shaking the cylinder, so immediately is the direction of travel. The reverse motion seemed to be favored for larger particles and less viscous liquids. Figure 8 shows the drift Reynolds number Re_d plotted as a function of Ω and Fr for the larger cones in a fluid with a lower viscosity. These cones drift in the direction opposite to the orientation of their tip. The two cones have the same surface area and different aspect ratios of 2:1 and 3:1.

DISTANCE OF PARTICLE FROM THE AXIS

An obvious concern in the interpretation of these data is the possibility of wall effects when the particles stabilize too close to the cylinder wall. While a precise measurement of the distance of the particles from the cylinder axis was not possible, an approximate estimate can be found by a force balance in the plane through the particle perpendicular to the axis of rotation. For the purposes of a rough estimate we assume that the same forces act on the particle as would act on a spherical bubble. Expressions for the forces on bubbles can be found in Refs. 3 and 2. The drag force is expressed in terms of a drag coefficient, for which we take the large Re limit $48/\mathrm{Re}_r$.[3] The inertial, or added mass, force has the usual expression in terms of a coefficient C_A for which we use the sphere value 1/2. For the lift force we use the high-Reynolds number expression of Ref. 4 with a lift coefficient C_L also equal to 1/2. In this way, as shown in Ref. 2, one finds

$$r_e \simeq \frac{R_b{}^2(\rho_l - \rho_b)g}{\rho_l \omega \sqrt{81\nu^2 + \frac{1}{4}R_b{}^4\omega^2}}. \tag{1}$$

Here ρ_l and ν are the liquid density and kinematic viscosity, and ρ_b the bubble or particle density. For small viscosity this relation reduces to $\rho_l r_e \omega^2 \simeq (\rho_l - \rho_b)g$, which expresses a balance between the centrifugal and gravitational pressure gradients. Similarly, when viscosity dominates, we find $\mu_l(\omega r_e)R_b \simeq R_b^3(\rho_l - \rho_b)g$, which balances the Stokes-type drag in a liquid with viscosity μ_l with buoyancy. Thus, while (1) may not rest on a particularly firm theoretical basis, it does embody the correct limiting behaviors and may offer a reasonable interpolation between the two for intermediate situations.

At large rotation rates, Eq. (1) shows that $\omega r_e \propto \omega^{-1}$. The proportionality of the drift velocity v_z to ω^{-2} pointed out before in connection with Fig. 7 would then be understandable if the force causing the drift were to scale like the square of the rotational velocity at the particle position as with a Bernoulli effect. For low rotation rates, on the other hand, Eq. (1) shows that the particle is closer to the cylinder wall and wall effects eventually may become dominant. The data for which the particles are estimated [with Eq. (1)] to be less than a particle diameter from the wall are indicated by open symbols in Figs. 6–8. While most of the data points falling away from the straight lines appear to correspond to locations affected by the proximity to the wall, others do not. Hence, whether the two regimes apparent from the figures are indeed to be ascribed to wall effects must remain an open question at present.

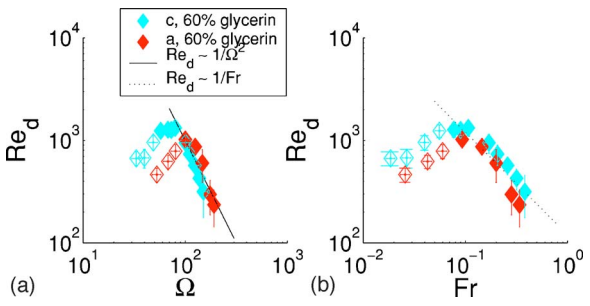

FIG. 8. Drift Reynolds number vs (a) Ω, and (b) Fr for cones moving away from the tip. Decreasing the viscosity or increasing the size of the particle can reverse the direction of drift.

A QUALITATIVE EXPLANATION

A qualitative explanation for the transverse motion can be found by considering the pressure distribution over the particle or bubble surface. When a fluid flows over an object, on the high velocity sides of the object surface the pressure is low causing suction forces. If the flow did not separate, a nonzero lift force would be generated since opposite surface

elements are not parallel to the axis. It is likely that a similar stress distribution is responsible for the phenomenon described before. Under the action of this lift force, the particle would drift axially at a velocity such that the drag balances the lift. In this sense the drift we have observed can be understood as analogous to the forward motion of a falling inclined cone, with the falling velocity replaced by the liquid rotation.

Mathematically, an equivalent description may be given in terms of the added mass tensor.[5] In the absence of fore-aft symmetry, the added mass tensor has nonzero off-diagonal elements when expressed in the cylindrical coordinates of the present situation. In particular, there will be a nonzero rz element with the result that a radial acceleration (in the present case the centrifugal acceleration) produces a force in the z direction. At low rotation rates the particle has more tilt with respect to the cylinder axis, the situation is more asymmetric, and the off-diagonal components of the tensors increase, giving rise to higher transverse velocities.

ACKNOWLEDGMENT

The work is part of the research program of FOM, which is financially supported by NWO.

[1] M. A. Naciri, "Contribution a l'etude des forces exercees par un liquide sur une bulle de gaz: Portance, masse ajoutee et interactions hydrodynamiques," Ph.D. thesis, L'Ecole Central de Lyon, 1992.
[2] D. Lohse and A. Prosperetti, "Controlling bubbles," J. Phys.: Condens. Matter **15**, S515 (2003).
[3] J. Magnaudet and I. Eames, "The motion of high-Reynolds number bubbles in inhomogeneous flows," Annu. Rev. Fluid Mech. **32**, 659 (2000).
[4] T. R. Auton, J. Hunt, and M. Prud'Homme, "The force excerted on a body in inviscid unsteady non-uniform rotating flow," J. Fluid Mech. **197**, 241 (1988).
[5] H. Lamb, *Hydrodynamics* (Cambridge University Press, Cambridge, 1932).